Design and control of an altazimuth liquid mirror telescope

Juan Cristobal Alcaraz Tapia[1], Carlos E. Castañeda[2], and Héctor Vargas-Rodríguez[3]

***Abstract*—In this paper, it is considered the design of a telescope in an altazimuth configuration. Its primary objective is a rotating liquid mirror made of mercury (any rotating liquid naturally adopts a perfect paraboloidal shape). This liquid mirror cannot be oriented. Hence, a mechanical and optical system is needed to conduct the light of a celestial body to it. The latter system is composed of two plane mirrors which, rotate around a horizontal and a vertical axis, two motors are employed to fulfill this purpose. The non-linear-block-control method is used to control these motors. A third motor keeps-up rotating a container filled with mercury to form the liquid mirror, the focal length of the rotating mirror depends on the angular velocity of this last motor. Hence, its rotation rate also needs to be controlled. The Methodology's part A describes the design of a 2-links mechanical and optical system. The Methodology's part B introduces the gravitational potential and the kinetic energy for each link in the mechanical and optical system. Then, using the Euler-Lagrange formalism, the equations governing this mechanical and optical system are obtained. Next, in the Methodology's part C, a nonlinear block control strategy is used to synthesize the control algorithm for the mechanical and optical guide system. Finally, a stability analysis is performed, using the Lyapunov criterion.**

The obtained results are presented via simulation using the software Simulink®.

***Index Terms*—Liquid mirror telescope, star tracking system, non-linear block control, telescope movement.**

I. Introduction

THERE have been various articles about liquid mirrors in the last 35 years since [1], which mentions the usefulness of these liquid mirrors in a telescope for a specific type of observations. This kind of applications is possible due to electro-optical tracking that, can be achieved thanks to the advent of charge-coupled devices (CCD) detectors. The firsts liquid mirror telescopes (LMT's) like the NASA's orbital debris observatory (NODO) [2] used CCD detectors, as well as the modern like the 4m International Liquid Mirror Telescope, will use [3]. LMT's were not taken seriously before using CCD's, because the liquid mirror cannot tilt in order to track a star. As a result, while stars move apparently in the sky, a film in the telescope register them as streaks. The use of a CCD detector solves this problem by moving its light sensors electronically from the east to the west, at a rate matching the drift of images in view of the telescope. This is equivalent to taking a picture with a photographic film that moves in a camera at the same speed as the image of a moving object. Tipically in only a couple of minutes, an object crosses the narrow width of the detector, limiting the amount of light that can be gathered. Observing the same region of the sky night after night, it is possible to create increasingly intense images by digitally adding subsequent exposures on a computer [4]. Even with its restriction to the zenith, Liquid Mirror Telescopes (LMT's) are still very appropriate for many survey applications, including large-scale structure, galaxy evolution, depth of a Quasi-stellar object (QSO), galaxy surveys, etc. Therefore, the LMT design is directed towards those applications which need large samplings of data, not necessarily from any specific direction in space [5]. The Large Zenith Telescope [6] is proof of this, it was built with a budget of more than an order of magnitude lower than that of conventional telescope projects of a comparable aperture. Even it has been presented the feasibility and scientifical potential of a 20-100 m aperture astronomical LMT constructed in one of the lunar poles [7]. And there are projects under development among them the Advanced Liquid-Mirror Probe for Astrophysics, Cosmology, and Asteroids (ALPACA) and the International Liquid-Mirror Telescope (ILMT) [6]. This last one is under construction.

On the other hand, when a container filled with a liquid is rotated, the pull of gravitational and centrifugal forces shapes the surface of the liquid into a perfect parabola [4]. The shape of the objectives in conventional telescopes is a parabola, so rotating a container with a reflecting liquid, such as mercury, results in a liquid mirror with a perfect shape for a telescope's objective. In fact in [8] the quality of astronomical images provided by the NODO and the LZT was assessed and compared to that of conventional instruments, concluding the images provided by the LMT's are of scientific quality.
The focal length l of the liquid mirror is given by:

$$l = \frac{g}{2\omega^2} \ , \tag{1}$$

for a given value of the acceleration of gravity g, the focal length is determined by the angular velocity ω [1]. As proved by Borra [4], the surface made by a liquid mirror can be perfectly parabolic and limited diffracted. There are other uses besides astronomical ones for a liquid mirror such as atmospheric science or in a telecentric F-Θ scanner with a low-cost liquid mirror objective [9].

II. Proposed methodology

A. Liquid mirror telescope design

As mentioned in the previous section, LMT's cannot tilt, and as a consequence, they cannot follow a celestial object in

J. C. Alcaraz, Carlos E. Castañeda and Héctor Vargas are with Departamento de Ciencias Exactas y Tecnología, Centro Universitario de los Lagos, Universidad de Guadalajara, MEX e-mail:[1]cristobal.alcaraz@alumnos.udg.mx, [2]ccastaneda@lagos.udg.mx, [3]hvargas@culagos.udg.mx.

the sky. In order to overcome this inconvenient, this subsection describes the design of an orientable LMT. Fig. 1 shows the main elements of the LMT and Table I lists every component shown in this figure.

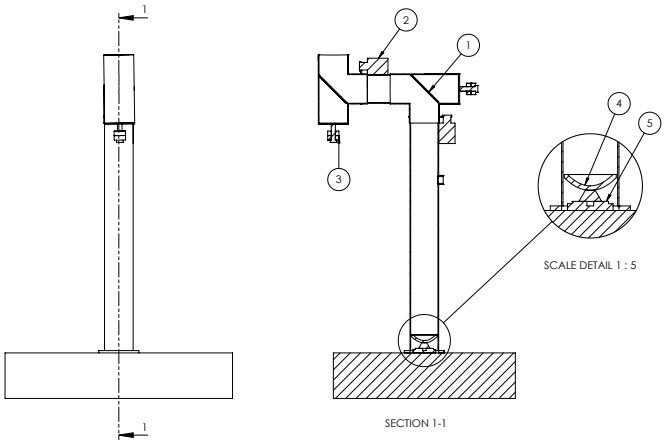

Fig. 1. Design and main elements of the tiltable LMT.

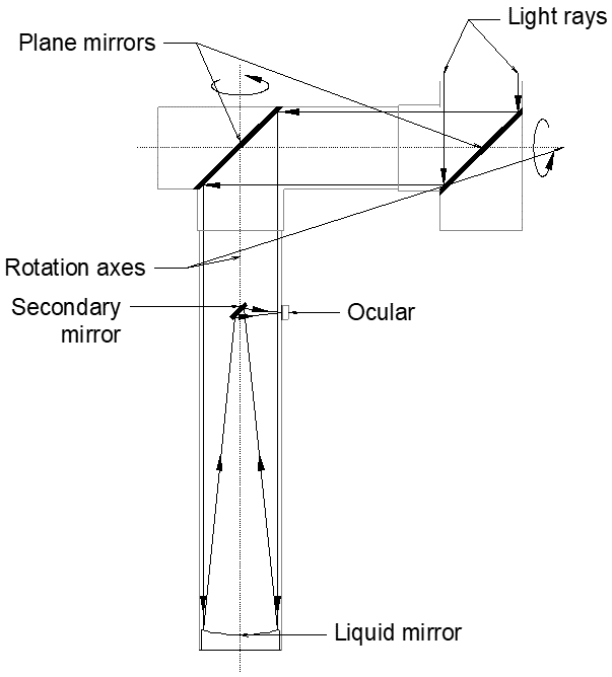

Fig. 2. Reflection of the light inside the telescope.

TABLE I
LIQUID MIRROR TELESCOPE'S MAIN COMPONENTS OF FIGURE 1.

No. of element	Piece	Quantity
1	Plane mirror	2
2	Motor	2
3	Counterweight	2
4	Container with liquid mercury	1
5	Air bearing	1

The two plane mirrors direct the light to the liquid mirror. One of these plane mirrors is rotating around the horizontal axis, while the other one around the vertical axis; both of them along with the pipe containing them. The sketch in Fig. 2 shows this path of the light inside the telescope from the source to the ocular. In this figure, the light is represented by rays in order to describe its path inside the telescope; first, the incoming light is reflected along the horizontal pipe, then the other flat mirror redirects the light to the liquid mirror. The plane mirrors are tilted $45°$ with respect to the pipes' axis, then vertical rays are reflected horizontally, and *vice versa*. Fig. 3 contains a 3d-model of the proposed design and the range of movement of the links of the telescope.

The coordinates of a star in the celestial sphere are called declination (δ) and right ascension (R.A.), these are known as equatorial coordinates [10]. The telescope proposed is in an altazimuth configuration, so, it is necessary to convert equatorial coordinates of the star (R.A. and δ) to horizon coordinates (q_1 and q_2 (Fig. 4)) of the telescope in order to track the reference (the movement of a star).

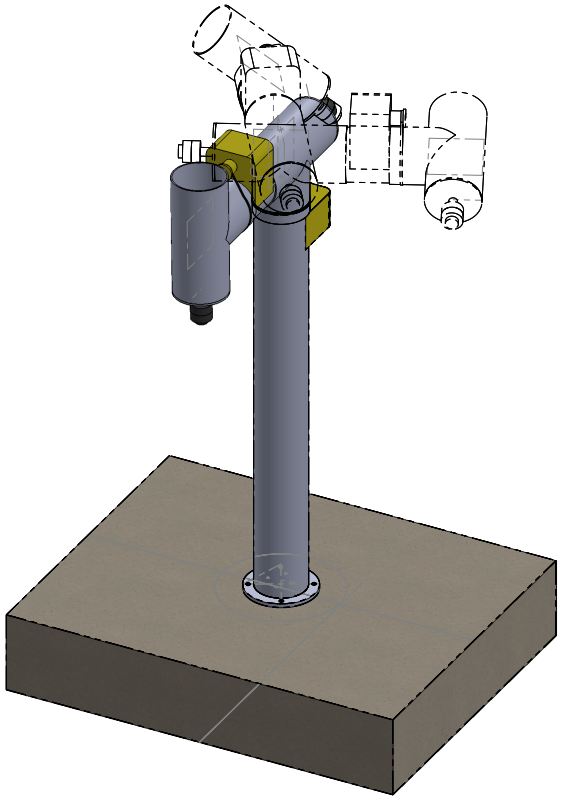

Fig. 3. Telescope's range of movement.

B. Kinematics and dynamics

Before we design a control strategy, it is necessary to have a dynamic model to which apply it for simulation purposes; in this case, the dynamic model of the telescope proposed. The present subsection describes the obtention of the dynamics,

by the use of the Euler-Lagrange equations. The function required to obtain the dynamics is the Lagrangian. This function is the difference between the kinetic and potential energy of the mechanical model of the proposed telescope. For the calculation of kinetic energy, the linear velocity of each link of the telescope is needed. The linear velocity is represented as a function of joint velocity, this function is known as differential kinematics, which is the derivative with respect to time of a function called direct kinematics. Direct kinematics is a function of the joint variable (q). So, before obtaining the dynamic model of the proposed telescope and to apply a control strategy, the direct kinematics and differential kinematics will be required.

1) Direct kinematics: The mechanical structure of the telescope proposed has $n = 2$ degrees of freedom, each one is associated with one joint articulation. Then, this subsection describes the direct kinematics of the proposed telescope. The aim of direct kinematics is to compute the position of the last link as a function of the joint variable [11]; that is, $f_R(q)$ where q is the joint variable. There are various methods to determine the direct kinematics model, but a first way to determine it is by applied geometry [11]. Another method is the Denavit-Hartenberg convention [12], which is more convenient for a greater number of degrees of freedom because is a systematic method. Using the last one mentioned, it is obtained the direct kinematics of the telescope's mechanic model shown in Fig. 4, using the symbolic values presented in Table II, where l_1 and l_2 are the lengths of links 1 and 2 starting from their rotation axes; B_1 is the offset from the origin of the inertial frame to the rotation axis of the link 2; B_2 is the distance from the end of link 1 to the center of link 2; q_1 and q_2 are the rotation angles of links 1 and 2, respectively; and α is the angle between the rotation axis for link 1 (Z_1) and the rotation axis for link 2 (Z_2). So, the Denavit-Hartenberg representation for link 1, through homogeneous transformations is as follows:

$$H_0^1 = R_{z,q_1} T_{z,d_1} T_{x,l_1} R_{x,\alpha_1} = \begin{bmatrix} \cos q_1 & 0 & \sin q_1 & l_1 \cos q_1 \\ \sin q_1 & 0 & -\cos q_1 & l_1 \sin q_1 \\ 0 & 1 & 0 & B_1 \\ 0 & 0 & 0 & 1 \end{bmatrix} \quad (2)$$

where R_{z,q_1} and R_{x,α_1} are rotation homogeneous transformation around axes Z and X of the link in question, respectively; T_{z,d_1} and T_{x,l_1} are translation homogeneous transformation; and H_0^1 is the homogeneous transformation relationing the coordinates in the reference system of link 1 and the reference system at the base of the telescope, as it is shown in Fig. 4 [13]. In equation (2), the rows 1-3 in the column 4, represent the position $[\mathrm{X}_0, \mathrm{Y}_0, \mathrm{Z}_0]^\top$ of the end of link 1 as follows:

$$\begin{bmatrix} \mathrm{X}_0 \\ \mathrm{Y}_0 \\ \mathrm{Z}_0 \end{bmatrix} = \begin{bmatrix} l_1 \cos q_1 \\ l_1 \sin q_1 \\ B_1 \end{bmatrix} . \quad (3)$$

Continuing with the Denavit-Hartenberg convention on link 2, we obtain $H_0^2 = H_1^2 H_0^1$. It is important to mention that the direct application of the Denavit-Hartenberg convention

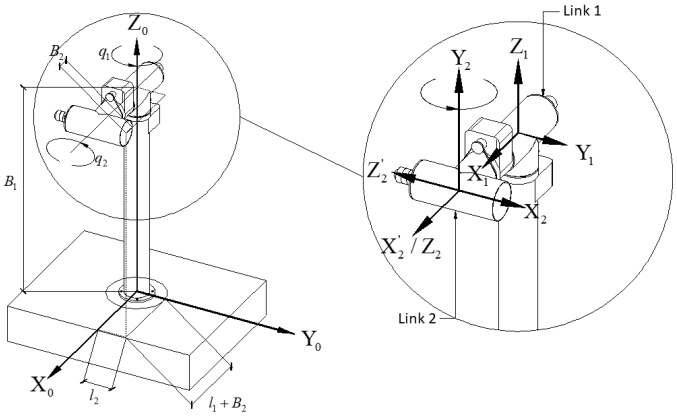

Fig. 4. Telescope's mechanic model

TABLE II
SYMBOLIC VALUES FOR THE PROPOSED TELESCOPE.

Link	Lenght (m)	Angle between rotation axes (rad)	Offset (m)	Rotation angles (rad)
1	l_1	$\frac{\pi}{2}$	B_1	q_1
2	l_2	0	B_2	q_2

for link 2 leads to the reference system $[\mathrm{X}_2', \mathrm{Y}_2, \mathrm{Z}_2']^\top$ shown in Fig. 4. This would be true if the two links were parallels because the X_1 and X_2 axes are along the length of their corresponding link. But links 1 and 2 form a right angle; so, in order to represent this configuration of links, it is necessary to rotate link 2 around the Y_2 axis an angle of $\frac{\pi}{2}$ rads. This conduces to the reference system of link 2 $[\mathrm{X}_2, \mathrm{Y}_2, \mathrm{Z}_2]^\top$. For the rotation, it is used a rotation homogeneous transformation around the axis Y_2; and the position vector for the end of link 2 is:

$$\begin{bmatrix} \mathrm{X}_0 \\ \mathrm{Y}_0 \\ \mathrm{Z}_0 \end{bmatrix} = \begin{bmatrix} B_2 \cos(q_1) + l_1 \cos(q_1) - l_2 \cos(q_2) \sin(q_1) \\ B_2 \sin(q_1) + l_1 \sin(q_1) + l_2 \cos(q_1) \cos(q_2) \\ B_1 + l_2 \sin(q_2) \end{bmatrix} . \quad (4)$$

Then, the direct kinematics of each link in the mechanic model of the proposed telescope is represented by equations (3) and (4), which are in function of the joint variables q_1 and q_2.

2) Differential kinematics: The differential kinematics gives the relationship between joint velocity $\dot{q}$ and the lineal velocity $\boldsymbol{v}$ [11], [14]; then:

$$\frac{d}{dt} \begin{bmatrix} \mathrm{X} \\ \mathrm{Y} \\ \mathrm{Z} \end{bmatrix} = \frac{d}{dt} \boldsymbol{f}_R(\boldsymbol{q}) = \frac{\partial \boldsymbol{f}_R(\boldsymbol{q})}{\partial \boldsymbol{q}} \dot{\boldsymbol{q}} = J(\boldsymbol{q}) \dot{\boldsymbol{q}} = \boldsymbol{v} , \quad (5)$$

where $[\mathrm{X\ Y\ Z}]^\top$ is the position vector as a function of the joint variable obtained by the direct kinematics (equations (3) and (4)), $J(q)$ is the Jacobian of the robot or analytical Jacobian [14], and $\boldsymbol{f}_R(\boldsymbol{q})$ is a function of the joint variable $\boldsymbol{q}$.

The lineal velocity $\boldsymbol{v}_1$ of the center of mass (cm) corresponding to the link 1 is obtained as follows:

$$\boldsymbol{v}_1 = \frac{d}{dt} \begin{bmatrix} l_{1\mathrm{cm}} \cos q_1 \\ l_{1\mathrm{cm}} \sin q_1 \\ B_1 \end{bmatrix} = \begin{bmatrix} -l_{1\mathrm{cm}} \sin q_1 \\ l_{1\mathrm{cm}} \cos q_1 \\ 0 \end{bmatrix} \dot{q}_1 . \quad (6)$$

The linear velocity of the center of mass corresponding to the link 2 is obtained as:

$$\begin{aligned}\boldsymbol{v}_2 &= \frac{d}{dt}\begin{bmatrix} B_2\cos q_1 + l_1\cos q_1 - l_{2\text{cm}}\cos q_2\sin q_1 \\ B_2\sin q_1 + l_1\sin q_1 + l_{2\text{cm}}\cos q_1\cos q_2 \\ B_1 + l_{2\text{cm}}\sin q_2 \end{bmatrix}, \\ &= \begin{bmatrix} v_{2\_11} & l_{2\text{cm}}\sin q_2\sin q_1 \\ v_{2\_21} & -l_{2\text{cm}}\cos q_1\sin q_2 \\ 0 & l_{2\text{cm}}\cos q_2 \end{bmatrix}\begin{bmatrix}\dot{q}_1 \\ \dot{q}_2\end{bmatrix}\end{aligned} \quad (7)$$

where $v_{2\_11} = -B_2\sin q_1 - l_1\sin q_1 - l_{2\text{cm}}\cos q_2\cos q_1$ and $v_{2\_21} = B_2\cos q_1 + l_1\cos q_1 - l_{2\text{cm}}\sin q_1\cos q_2$.
Equations (6) and (7) represent the linear velocity for links 1 and 2, respectively; now, it is possible to compute the kinetic energy needed for the dynamics, which it is shown in section II-B3.

3) Dynamics: Now, it is necessary to determine the equations of motion of the proposed telescope design; this is in order to propose control strategies that can be tested for simulation purposes. The method chosen in this paper to determine the dynamic equations of the telescope is the use of the Euler-Lagrange equations. In order to determine the Euler-Lagrange equations, it is necessary to obtain the Lagrangian of the system, which is the difference between the kinetic energy and the potential energy [15] as follows:

$$\mathcal{L}(\boldsymbol{q},\dot{\boldsymbol{q}}) = \mathcal{K}(\boldsymbol{q},\dot{\boldsymbol{q}}) - \mathcal{U}(\boldsymbol{q}) \quad (8)$$

where $\mathcal{L}(\boldsymbol{q},\dot{\boldsymbol{q}})$ is the Lagrangian, $\mathcal{K}(\boldsymbol{q},\dot{\boldsymbol{q}})$ is the kinetic energy, and $\mathcal{U}(q)$ the potential energy.

It is important to mention that the proposed telescope has the configuration of the two degrees of freedom (DOF) robot manipulator. Then, the Euler-Lagrange equation of motion for the n DOF is:

$$\frac{d}{dt}\left[\frac{\partial\mathcal{L}(\boldsymbol{q},\dot{\boldsymbol{q}})}{\partial\dot{\boldsymbol{q}}}\right] - \frac{\partial\mathcal{L}(\boldsymbol{q},\dot{\boldsymbol{q}})}{\partial\boldsymbol{q}} = \boldsymbol{\tau} - \boldsymbol{f}_f(\dot{\boldsymbol{q}},\boldsymbol{f}_e) \quad (9)$$

The equation (9) can be written in the following form:

$$\boldsymbol{\tau} = \mathrm{M}(\boldsymbol{q})\ddot{\boldsymbol{q}} + \dot{\mathrm{M}}(\boldsymbol{q})\dot{\boldsymbol{q}} - \frac{\partial}{\partial\boldsymbol{q}}\left[\frac{1}{2}\dot{\boldsymbol{q}}^\top\mathrm{M}(\boldsymbol{q})\dot{\boldsymbol{q}}\right] + \frac{\partial\mathcal{U}(\boldsymbol{q})}{\partial\boldsymbol{q}} + \boldsymbol{f}_f(\dot{\boldsymbol{q}},\boldsymbol{f}_e), \quad (10)$$

which, in its compact form and with the most widely used notation in the area of robotics [14], [11] is described as follows:

$$\boldsymbol{\tau} = \mathrm{M}(\boldsymbol{q})\ddot{\boldsymbol{q}} + \mathrm{C}(\boldsymbol{q},\dot{\boldsymbol{q}})\dot{\boldsymbol{q}} + \boldsymbol{G}(\boldsymbol{q}) + \boldsymbol{f}_f(\dot{\boldsymbol{q}},\boldsymbol{f}e), \quad (11)$$

where $\boldsymbol{\tau}\in\mathbb{R}^n$ is the vector of applied torques, $\boldsymbol{q}\in\mathbb{R}^n$ is the vector of generalized coordinates or joint positions, $\dot{\boldsymbol{q}}\in\mathbb{R}^n$ is the vector of joint velocities and $\ddot{\boldsymbol{q}}\in\mathbb{R}^n$ is the vector of joint accelerations. $\mathrm{M}(\boldsymbol{q})\in\mathbb{R}^{n\times n}$ is the inertia matrix, which is symmetric and positive definite, $\mathrm{C}(\boldsymbol{q},\dot{\boldsymbol{q}})\in\mathbb{R}^{n\times n}$ is the matrix of centripetal and Coriolis forces, which is defined as follows:

$$\mathrm{C}(\boldsymbol{q},\dot{\boldsymbol{q}})\dot{\boldsymbol{q}} = \dot{\mathrm{M}}(\boldsymbol{q})\dot{\boldsymbol{q}} - \frac{\partial}{\partial\boldsymbol{q}}\left[\frac{1}{2}\dot{\boldsymbol{q}}^\top\mathrm{M}(\boldsymbol{q})\dot{\boldsymbol{q}}\right],$$

$\boldsymbol{G}(\boldsymbol{q})\in\mathbb{R}^n$ is the vector of gravitational forces obtained as the gradient of the potential energy, this is:

$$\boldsymbol{G}(\boldsymbol{q}) = \frac{\partial\mathcal{U}(\boldsymbol{q})}{\partial\boldsymbol{q}},$$

and $\boldsymbol{f}_f(\dot{\boldsymbol{q}},\boldsymbol{f}_e)\in\mathbb{R}^n$ is the vector of friction forces that includes the viscous, Coulomb and static friction ($\boldsymbol{f}_e$) of each articulation.

The function $\mathcal{K}(\boldsymbol{q},\dot{\boldsymbol{q}})$ includes rotational and translational kinetic energy [14]:

$$\mathcal{K}_i(\boldsymbol{q},\dot{\boldsymbol{q}}) = \frac{1}{2}m_i\boldsymbol{v}_i^\top\boldsymbol{v}_i + \frac{1}{2}I_i\left[\sum_i^n\dot{\boldsymbol{q}}_i\right]^2, \quad i=1,...,n, \quad (12)$$

with $n=2$ as the number of DOF, and where m_i and I_i are the mass and moment of inertia of the i-th, respectively. The moment of inertia of the i-th link is around an axis that passes through its center of mass and is parallel to the rotation axis around which the link rotates [15].
Then, using the equation (12), the kinetic energies for link 1 and link 2 are:

$$\mathcal{K}_1 = \frac{1}{2}m_1\boldsymbol{v}_1^\top\boldsymbol{v}_1 + \frac{1}{2}I_1\dot{q}_1^2\ , \quad (13)$$

$$\mathcal{K}_2 = \frac{1}{2}m_2\boldsymbol{v}_2^\top\boldsymbol{v}_2 + \frac{1}{2}I_2(\dot{q}_1+\dot{q}_2)^2. \quad (14)$$

From equations (6) and (7), it can be obtained $\boldsymbol{v}_1^\top\boldsymbol{v}_1$ and $\boldsymbol{v}_2^\top\boldsymbol{v}_2$, respectively as:

$$\boldsymbol{v}_1^\top\boldsymbol{v}_1 = (l_{1\text{cm}}\dot{q}_1)^2, \quad (15)$$

$$\begin{aligned}\boldsymbol{v}_2^\top\boldsymbol{v}_2 = {} & [(B_2\cos(q_1) + l_1\cos(q_1) - l_{2\text{cm}}\cos(q_2)\sin(q_1))\dot{q}_1 \\ & (-l_{2\text{cm}}\cos(q_1)\sin(q_2)\dot{q}_2)]^2 \\ & + [B_2\sin(q_1) + l_1\sin(q_1) + l_{2\text{cm}}\cos(q_1)\cos(q_2)\dot{q}_1 \\ & - l_{2\text{cm}}\sin(q_1)\sin(q_2)\dot{q}_2]^2 \\ & + [l_{2\text{cm}}\cos(q_2)\dot{q}_2].\end{aligned} \quad (16)$$

The total kinetic energy is:

$$\mathcal{K}(\boldsymbol{q},\dot{\boldsymbol{q}}) = \mathcal{K}_1 + \mathcal{K}_2. \quad (17)$$

Unlike the kinetic energy, the potential energy does not have a specific form. It depends on the geometry of the robot (for our particular case, the proposed telescope). The potential energy for links 1 and 2 is:

$$\mathcal{U}_1 = m_1 g B_1, \quad (18)$$

$$\mathcal{U}_2 = m_2 g(B_1 + l_{2\text{cm}}\sin q_2). \quad (19)$$

The total potential energy is:

$$\mathcal{U}(\boldsymbol{q}) = \mathcal{U}_1 + \mathcal{U}_2. \quad (20)$$

In order to obtain the Lagrangian, the kinetic (17) and potential (20) energy are substitued in equation (8), and the Euler-Lagrange's equation of motion (9) can be obtained. The result can be represented as in equation (11), where the entries of the inertia matrix $\mathrm{M}(\cdot)$ are:

$$\begin{aligned}M_{11} &= I_1 + I_2 + l_1^2 m_2 + l_{1_{cm}}^2 m_1 \\ &\quad + B_2^2 m_2 + l_{2\text{cm}}^2 m_2\cos^2(q_2) + 2B_2 l_1 m_2 \\ M_{12} &= I_2 - B_2 l_{2\text{cm}} m_2\sin(q_2) - l_1 l_{2\text{cm}} m_2\sin(q_2) \\ M_{21} &= I_2 - B_2 l_{2\text{cm}} m_2\sin(q_2) - l_1 l_{2\text{cm}} m_2\sin(q_2) \\ M_{22} &= I_2 + l_{2\text{cm}}^2 m_2.\end{aligned} \quad (21)$$

The entries in the matrix of centripetal and Coriolis forces $\mathrm{C}(\cdot)$ are:

$$\begin{aligned} C_{11} &= -(l_{2\mathrm{cm}}^2 m_2 \sin(2q_2)\dot{q}_2) \\ C_{12} &= [-B_2 l_{2\mathrm{cm}} m_2 \cos(q_2) - l_1 l_{2\mathrm{cm}} m_2 \cos(q_2)]\,\dot{q}_2 \\ C_{21} &= l_{2\mathrm{cm}}^2 m_2 \cos(q_2)\sin(q_2)\dot{q}_1 \\ C_{22} &= 0. \end{aligned} \tag{22}$$

The entries in the vector of gravitational forces $\boldsymbol{G}(\cdot)$ are:

$$\begin{aligned} G_{11} &= 0 \\ G_{21} &= g l_{2\mathrm{cm}} m_2 \cos(q_2). \end{aligned} \tag{23}$$

The entries in the vector of friction forces $\boldsymbol{f}_f(\cdot)$ are:

$$\begin{bmatrix} f_{f1}(\dot{q}_1, f_{e1}) \\ f_{f2}(\dot{q}_2, f_{e2}) \end{bmatrix} = B\dot{\boldsymbol{q}} + F_c\ \mathrm{sign}(\dot{\boldsymbol{q}}) + \begin{bmatrix} 1-|\mathrm{sign}(\dot{q}_1)| & 0 \\ 0 & 1-|\mathrm{sign}(\dot{q}_2)| \end{bmatrix} \boldsymbol{f}_e \tag{24}$$

where B and $F_c \in \mathbb{R}^{n\times n}$ are diagonal matrices with viscous and Coulomb friction coefficient, respectively. $\boldsymbol{f}_e$ is the vector of static friction and $\mathrm{sign}(\dot{\boldsymbol{q}}) = [\mathrm{sign}(\dot{q}_1),\ \mathrm{sign}(\dot{q}_2)]^\top$.
Then, the dynamic equations of the model of the telescope can be represented in the state space as follows:

$$\begin{aligned} \begin{bmatrix} \dot{x}_1 \\ \dot{x}_2 \end{bmatrix} &= \begin{bmatrix} x_3 \\ x_4 \end{bmatrix} \\ \begin{bmatrix} \dot{x}_3 \\ \dot{x}_4 \end{bmatrix} &= \mathcal{N}\left[\boldsymbol{U} - C\begin{bmatrix} x_3 \\ x_4 \end{bmatrix} - \boldsymbol{G} - \boldsymbol{f}_f\right], \end{aligned} \tag{25}$$

where

$$\mathcal{N} = \mathrm{M}^{-1}, \quad \begin{bmatrix} x_1 \\ x_2 \\ x_3 \\ x_4 \end{bmatrix} = \begin{bmatrix} q_1 \\ q_2 \\ \dot{q}_1 \\ \dot{q}_2 \end{bmatrix}, \quad \boldsymbol{U} = \begin{bmatrix} u_1 \\ u_2 \end{bmatrix} = \begin{bmatrix} \tau_1 \\ \tau_2 \end{bmatrix}.$$

Now, with the dynamic equation of the proposed telescope represented in state space (25), a strategy of control can be applied.

C. Control design

In this section, it is proposed a non-linear block control algorithm in order to the telescope tracks a star movement.

1) Telescope control design: For this paper, model (25) can be represented as a non-linear block controllable form (NBC-form) [16], which is represented by two blocks:

$$\begin{aligned} \dot{\mathcal{X}}^1 &= \mathcal{X}^2 \\ \dot{\mathcal{X}}^2 &= f^2(\mathcal{X}^1, \mathcal{X}^2) + \mathcal{D}(\mathcal{X}^1)\boldsymbol{U} \end{aligned} \tag{26}$$

where

$$\mathcal{X}^1 = \begin{bmatrix} x_1 \\ x_2 \end{bmatrix},\ \mathcal{X}^2 = \begin{bmatrix} x_3 \\ x_4 \end{bmatrix}, \tag{27}$$

$$\begin{aligned} f^2(\cdot) &= \mathcal{N}\left[-C\begin{bmatrix} x_3 \\ x_4 \end{bmatrix} - \boldsymbol{G} - \boldsymbol{f}_f\right] \\ &= \begin{bmatrix} \mathcal{N}_{11}\left[-C_{11}x_3 - C_{12}x_4 - G_{11} - f_{f1}\right] \\ \mathcal{N}_{21}\left[-C_{11}x_3 - C_{12}x_4 - G_{11} - f_{f1}\right] \\ +\mathcal{N}_{12}\left[-C_{21}x_3 - G_{21} - f_{f2}\right] \\ +\mathcal{N}_{22}\left[-C_{21}x_3 - G_{21} - f_{f2}\right] \end{bmatrix}, \end{aligned} \tag{28}$$

and

$$\mathcal{D}(\cdot) = \mathcal{N} \tag{29}$$

The error $\mathcal{E}^1$ ($\mathcal{E}^2$) is the difference between the block $\mathcal{X}^1$ ($\mathcal{X}^2$) (27) and the reference signal to be tracked $\mathcal{X}_d^1$ ($\mathcal{X}_d^2$). Note that signals $\mathcal{X}_d^1$ and $\mathcal{X}_d^2$ are the joint angle and joint velocity of each link of the telescope, respectivaly, needed to keep a star in sight. Then $\mathcal{E}^1$ and $\mathcal{E}^2$ are represented as follows:

$$\mathcal{E}^1 = \mathcal{X}^1 - \mathcal{X}_d^1, \tag{30}$$

$$\mathcal{E}^2 = \mathcal{X}^2 - \mathcal{X}_d^2, \tag{31}$$

where

$$\mathcal{X}_d^1 = \begin{bmatrix} x_{1d} \\ x_{2d} \end{bmatrix} = \begin{bmatrix} 270 - A \\ a \end{bmatrix}, \tag{32}$$

and

$$\begin{bmatrix} a \\ A \end{bmatrix} = \begin{bmatrix} \sin^{-1}(\sin\delta\sin\phi + \cos\delta\cos\phi\cos H) \\ \cos^{-1}\left(\dfrac{\sin\delta - \sin\phi\sin a}{\cos\phi\cos a}\right) \end{bmatrix}. \tag{33}$$

The equation (33) shows the relation between the hour-angle H, the declination δ, the observer's geographical latitude ϕ, the azimuth A, and the altitude a [17], and $\mathcal{X}_d^2 = [x_{3d}\ x_{4d}]^\top$. The azimuth angle A increases in the opposite way of q_1, starting from the north. If "X" in Fig. 4 points to the north, then, when the angle $q_1 = 0$, the link 2 of the telescope points to the west (axis Y). Taking this into account, it is easy to obtain the relation between these angles ($q_1 = 270°$-A).

The dynamics of $\mathcal{E}^1$ and $\mathcal{E}^2$ is:

$$\dot{\mathcal{E}}^1 = \dot{\mathcal{X}}^1 - \dot{\mathcal{X}}_d^1, \tag{34}$$

$$\dot{\mathcal{E}}^2 = \dot{\mathcal{X}}^2 - \dot{\mathcal{X}}_d^2. \tag{35}$$

Substituting the first equation of (26) in (34), yields:

$$\dot{\mathcal{E}}^1 = \mathcal{X}^2 - \dot{\mathcal{X}}_d^1. \tag{36}$$

Imposing the desired dynamics $K^1\mathcal{E}^1$ in (36), by choosing the desired value for the virtual control $\mathcal{X}_d^2$ [18], it is obtained:

$$K^1\mathcal{E}^1 = \mathcal{X}_d^2 - \dot{\mathcal{X}}_d^1. \tag{37}$$

Then

$$\mathcal{X}_d^2 = K^1\mathcal{E}^1 + \dot{\mathcal{X}}_d^1. \tag{38}$$

The time derivative of $\mathcal{X}_d^2$ is described by the following equation:

$$\dot{\mathcal{X}}_d^2 = K^1\dot{\mathcal{E}}^1 + \ddot{\mathcal{X}}_d^1. \tag{39}$$

Taking the value of $\mathcal{X}^2$ in (31), and the value of $\mathcal{X}_d^2$ in (38), and substituting them in (36), it is obtained:

$$\begin{aligned} \dot{\mathcal{E}}^1 &= \mathcal{E}^2 + \mathcal{X}_d^2 - \dot{\mathcal{X}}_d^1 \\ &= K^1\mathcal{E}^1 + \mathcal{E}^2. \end{aligned} \tag{40}$$

Now, for the dynamics of $\dot{\mathcal{E}}^2$, substituting $\dot{\mathcal{X}}^2$, $\mathcal{X}_d^2$, $\dot{\mathcal{X}}_d^2$, $\mathcal{X}^1$, $\mathcal{X}^2$ and $\dot{\mathcal{E}}^1$ from equations (26), (38), (39), (30), (31) and (40), respectively in equation (35), it is obtained:

$$\begin{aligned}\dot{\mathcal{E}}^2 &= \dot{\mathcal{X}}^2 - \dot{\mathcal{X}}_d^2 \\ &= f^2(\mathcal{X}^1, \mathcal{X}^2) + \mathcal{D}(\mathcal{X}^1)\boldsymbol{U} - \dot{\mathcal{X}}_d^2 \\ &= f^2(\mathcal{E}^1 + \mathcal{X}_d^1, \mathcal{E}^2 + \mathcal{X}_d^2) + \mathcal{D}(\mathcal{E}^1 + \mathcal{X}_d^1)\boldsymbol{U} - K^1\dot{\mathcal{E}}^1 - \ddot{\mathcal{X}}_d^1 \\ &= f^2(\mathcal{E}^1 + \mathcal{X}_d^1, \mathcal{E}^2 + K^1\mathcal{E}^1 + \dot{\mathcal{X}}_d^1) + \mathcal{D}(\mathcal{E}^1 + \mathcal{X}_d^1)\boldsymbol{U} \\ &\quad - K^1(K^1\mathcal{E}^1 + \mathcal{E}^2) - \ddot{\mathcal{X}}_d^1.\end{aligned} \tag{41}$$

The equation of system (26) is transformed to the block controllable form using the error dynamics as follows:

$$\begin{aligned}\dot{\mathcal{E}}^1 &= K^1\mathcal{E}^1 + \mathcal{E}^2 \\ \dot{\mathcal{E}}^2 &= f^2(\mathcal{E}^1 + \mathcal{X}_d^1, \mathcal{E}^2 + K^1\mathcal{E}^1 + \dot{\mathcal{X}}_d^1) + \mathcal{D}(\mathcal{E}^1 + \mathcal{X}_d^1)\boldsymbol{U} \\ &\quad - K^1(K^1\mathcal{E}^1 + \mathcal{E}^2) - \ddot{\mathcal{X}}_d^1.\end{aligned} \tag{42}$$

Then, imposing the desired dynamics for $\dot{\mathcal{E}}^2 = K^2\mathcal{E}^2$ in (41), the control signal $\boldsymbol{U}$ is defined by:

$$\begin{aligned}\boldsymbol{U} =& M(\mathcal{E}^1 + \mathcal{X}_d^1)\Big[-f^2(\mathcal{E}^1 + \mathcal{X}_d^1, \mathcal{E}^2 + K^1\mathcal{E}^1 + \dot{\mathcal{X}}_d^1) \\ &+ K^1(K^1\mathcal{E}^1 + \mathcal{E}^2) + \ddot{\mathcal{X}}_d^1 + K^2\mathcal{E}^2\Big].\end{aligned} \tag{43}$$

As it can be seen in equation (43), the control law $\boldsymbol{U}$ is in function of the errors $\mathcal{E}^1$ (30), $\mathcal{E}^2$ (31), and the desired reference $\mathcal{X}_d^1$ (32) including its first and second time derivatives ($\dot{\mathcal{X}}_d^1$ and $\ddot{\mathcal{X}}_d^1$). For the particular case of the present proposal, this reference signal varies in time due to the apparent movement of the stars in the sky, so, these derivatives exist. In fact, the first derivative is the rotation rate for each motor that controls the rotation of each link, and the second derivative is its angular acceleration.

2) Angular velocity control of the liquid mirror motor: As mentioned earlier, for varying the focal length of a liquid mirror, it is necessary to control the angular velocity of the recipient that contains the liquid mirror. The equation (1) represents the relation between angular velocity and the focal length. So, it is needed to apply a control algorithm to the model of a motor, which has to keep rotating the container mentioned at a constant velocity. In this work, the tracking of the angular velocity of the motor is accomplished by the use of the state-feedback linearization technique applied to a DC motor model, just as it is shown in reference [19]. This is in order to keep the focal length of the mirror in a desired value depending on the observations that will be done with the telescope.

D. Stability analysis

For the stability analysis, it is used the state space equation in terms of the errors $(\mathcal{E}^1, \mathcal{E}^2)$. This state space equation is represented by equation (40), and the result of substitute the control law (43) in (41) yields the following linear representation in state space:

$$\begin{aligned}\dot{\mathcal{E}}^1 &= K^1\mathcal{E}^1 + \mathcal{E}^2 \\ \dot{\mathcal{E}}^2 &= K^2\mathcal{E}^2\end{aligned} = \begin{bmatrix}K^1 & 1 \\ 0 & K^2\end{bmatrix}\begin{bmatrix}\mathcal{E}^1 \\ \mathcal{E}^2\end{bmatrix} \tag{44}$$

Each row in equation (44) is a block, so expanding each of these, results in:

$$\begin{bmatrix}\dot{\mathcal{E}}_1 \\ \dot{\mathcal{E}}_2 \\ \dot{\mathcal{E}}_3 \\ \dot{\mathcal{E}}_4\end{bmatrix} = \begin{bmatrix}k_1 & 0 & 1 & 0 \\ 0 & k_2 & 0 & 1 \\ 0 & 0 & k_3 & 0 \\ 0 & 0 & 0 & k_4\end{bmatrix}\begin{bmatrix}\mathcal{E}_1 \\ \mathcal{E}_2 \\ \mathcal{E}_3 \\ \mathcal{E}_4\end{bmatrix} \tag{45}$$

then, as it is explained in [20], the origin is asymptotically stable if $\mathrm{Re}\lambda_i < 0$ for all eigenvalues of the state matrix in (45); this is, the state matrix in (45) is a Hurwitz matrix or stability matrix. The eigenvalues of the state matrix in (45) are:

$$\begin{aligned}\lambda_1 &= k_1 \\ \lambda_2 &= k_2 \\ \lambda_3 &= k_3 \\ \lambda_4 &= k_4.\end{aligned} \tag{46}$$

The coefficients k_1, k_2, k_3, k_4 comes from:

$$K^1 = \begin{bmatrix}k_1 & 0 \\ 0 & k_2\end{bmatrix}, \quad K^2 = \begin{bmatrix}k_3 & 0 \\ 0 & k_4\end{bmatrix}$$

For a linear equation system like (45), it is considered the following quadratic Lyapunov function candidate [20]:

$$V(x) = x^\top P x \tag{47}$$

The derivative of (47) is given by:

$$\dot{V}(x) = x^\top P\dot{x} + \dot{x}^\top P x = -x^\top Q x \tag{48}$$

where Q is defined by:

$$PA' + A'^\top P = -Q \tag{49}$$

Then, a matrix A' is Hurwitz if and only if for any given positive definite symmetric matrix Q there exists a positive definite symmetric matrix P that satisfies the Lyapunov equation (49). Moreover, if A' is Hurwitz, then, the matrix P is unique [20]. Choosing Q as a real symmetric positive definite matrix (in this case the identity matrix), and solving for P, it is obtained:

$$P = \begin{bmatrix} -\frac{1}{2k_1} & 0 & \frac{1}{2k_1(k_1+k_3)} & 0 \\ 0 & -\frac{1}{2k_2} & 0 & \frac{1}{2k_2(k_2+k_4)} \\ \frac{1}{2k_1(k_1+k_3)} & 0 & P_{3,3} & 0 \\ 0 & \frac{1}{2k_2(k_2+k_4)} & 0 & P_{4,4} \end{bmatrix} \tag{50}$$

with:

$$P_{3,3} = -\frac{k_1^2 + k_1k_3 + 1}{2k_1k_3(k_1+k_3)} \text{and} \qquad P_{4,4} = -\frac{k_2^2 + k_2k_4 + 1}{2k_2k_4(k_2+k_4)}.$$

The matrix P (50) is positive definite if and only if all its leading principal minors are positive (which it is true if the values of k_1, k_2, k_3, k_4 are negative), and since Q is also definite positive we can conclude that the origin is asymptotically stable [20].

III. Results

A. Direct kinematics

Focusing only on link 1, it is easy to verify that the position vector (3) is correct, without the need of using the Denavit-Hartenberg convention. Link 1 rotates around a vertical axis Z, then its height does not vary, its position X is equal to the product of the length from the origin to the end of the link and the cosine of the angle q_1; thus, the position Y is equal to the product of the length l_1 and the sine of q_1. The position vector (4) is a little more complex to analyse, but it is more clear with the Figs. 5 and 6 and using the following values: $l_1 = l_2 = 0.10\ m$, $B_1 = 1.00\ m$ and $B_2 = 0.05\ m$ for different angles q_1 and q_2.

Figs. 5 and 6 show that when the angle q_1 turns a complete turn and the angle q_2 is fixed (Fig. 5), the end of link 2 starts on an X position $l_1 + B_2 = 0.15\ m$, a Y position $l_2 = 0.1\ m$, and the Z position does not change (stays in $B_1 = 1.00\ m$). Now, when q_1 is fixed and q_2 turns a complete turn (Fig. 6), the position X does not change (stays in $l_1 + B_2 = 0.15\ m$), the Y position reaches a maximum and minimum of $l_2 = 0.10\ m$ and $-l_2 = -0.10\ m$, respectively, and the Z position reaches a maximum and minimum value of $B_1 \pm l_2 = 1.00\ m \pm 0.1\ m$, respectively. These values correspond to the positions X, Y, and Z of the end of link 2, as it is shown in Fig. 4.

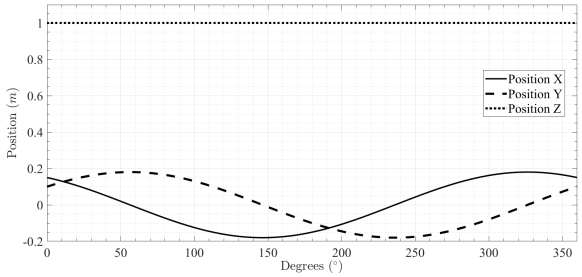

Fig. 5. Position X, Y and Z: q_1 turns a complete turn and q_2 is fixed.

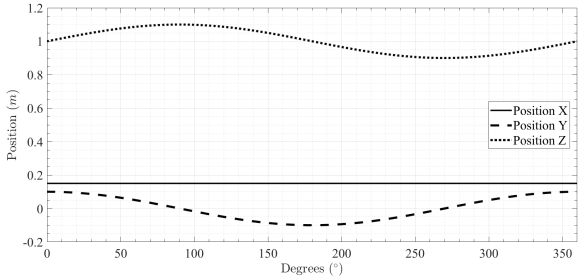

Fig. 6. Position X, Y and Z: q_1 is fixed and q_2 turns a complete turn.

B. Star tracking performance

By applying the Non-linear block control for the telescope's dynamic model, thus, using the control input vector obtained in equation (43), a signal reference (in this case the movement of a star (32)) can be tracked. It is required this reference ($\mathcal{X}_d^1$), its derivative ($\dot{\mathcal{X}}_d^1$), and second derivative ($\ddot{\mathcal{X}}_d^1$). The entries of equation (32) are the desired angles q_1 and q_2 for the links 1 and 2, respectively, needed for tracking a star.

In this work it is used the data for the star Altair (R.A.$=$ 19h 50min 47sec, $\delta = 8°52'6''$) [21] in order to be tracked by the telescope proposed. The observation is considered from a place with latitude $21.36°$, starting the tracking when the star is at the observer's zenith and for 4 hours (sidereal time). Figs. 7 and 8 show the tracking performance for angles q_1 and q_2, respectively. In both figures there is a detail that includes 10 seconds (sidereal time) of simulation, demonstrating the fast convergence given in two seconds approximately.

The signal references (x_{1d} and x_{2d} (32)) from Figs. 7 and 8, are obtained by converting equatorial to horizon coordinates, as it is explained in [17].

It is important to mention that the time in the graphics is sidereal time, and each hour-angle corresponds to 15 degrees from the observer's zenith to the star being observed. Then, 24 hours-angle corresponds to 360 degrees. The simulation time of Figs. 7 and 8 correspond to 3h 59min 20sec of solar time.

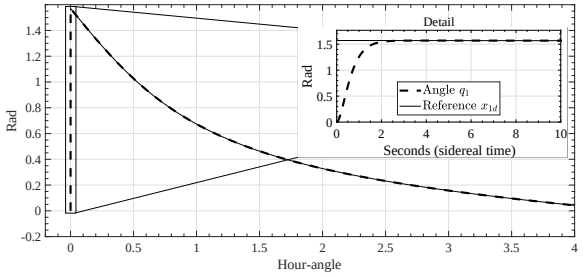

Fig. 7. Angular position tracking performance for q_1.

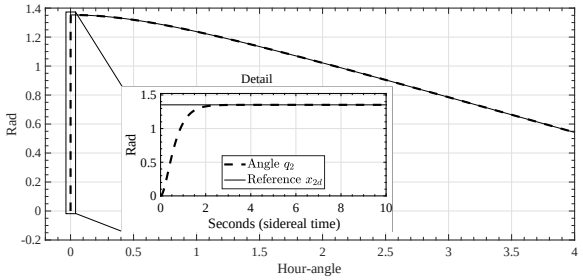

Fig. 8. Angular position tracking performance for q_2.

C. Liquid mirror's focal length tracking performance

As mentioned above, the liquid mirror in the telescope varies its focal length along with its angular velocity in a relationship described by equation (1). So, in order to keep a steady focal length, it is necessary to maintain a steady velocity.

Fig. 9 shows the control of the rotation of a DC motor tracking the angular velocity (reference) needed to maintain a focal

length of 1 m using the state-feedback linearization technique, applied to the DC motor model that is shown in [19].

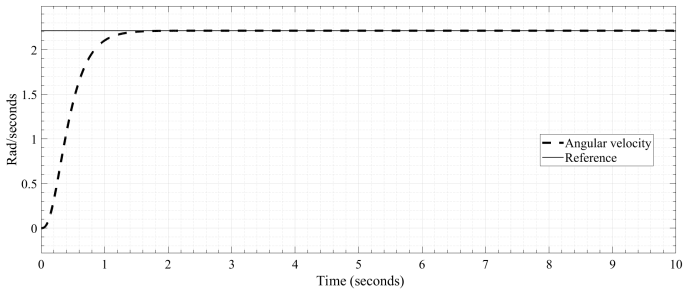

Fig. 9. Angular velocity tracking performance.

IV. Conclusion

Liquid mirror telescopes are a good alternative to conventional telescopes for a certain kind of observations, where it is not necessary to follow an astronomical object. Its mirror is relatively easy to form and does not require the careful precision the solid mirrors need in its ground and polished. But, they cannot be used to track an object in the sky. So, the configuration of the telescope presented in this paper along the control of the rotation of its links permits to overcome this disadvantage, allowing it to follow the position of a star. Directing the light of any astronomical object in sight, by means of two plane mirrors to a liquid mirror, which is the objective of the telescope.

Acknowledgment

Authors thanks to CONACYT (México) under scholarship number 779292 and to retention program 120489.

References

[1] E. F. Borra, "The liquid-mirror telescope as a viable astronomical tool," *Journal of the Royal Astronomical Society of Canada*, vol. 76, pp. 245–256, 1982.

[2] R. A. Cabanac, E. F. Borra, and M. Beauchemin, "A search for peculiar objects with the nasa orbital debris observatory 3 meter liquid mirror telescope," *The Astrophysical Journal*, vol. 509, no. 1, p. 309, 1998.

[3] J. Surdej and D. Mawet, "The 4m international liquid mirror telescope (ilmt)." Society of Photo-Optical Instrumentation Engineers (SPIE), 2006.

[4] E. F. Borra, "Liquid mirrors," *Scientific American*, vol. 270, p. 76, 1994.

[5] B. K. Gibson, "Liquid mirror telescopes-history," *Journal of the Royal Astronomical Society of Canada*, vol. 85, p. 158, 1991.

[6] P. Hickson, T. Pfrommer, R. Cabanac, A. Crotts, B. Johnson, V. De Lapparent, K. M. Lanzetta, S. Gromoll, M. K. Mulrooney, S. Sivanandam *et al.*, "The large zenith telescope: A 6 m liquid-mirror telescope," *Publications of the Astronomical Society of the Pacific*, vol. 119, no. 854, p. 444, 2007.

[7] R. Angel, D. Eisenstein, S. Sivanandam, S. P. Worden, J. Burge, E. Borra, C. Gosselin, O. Seddiki, P. Hickson, K. B. Ma *et al.*, "A lunar liquid mirror telescope (llmt) for deep-field infrared observations near the lunar pole," in *SPIE Astronomical Telescopes+ Instrumentation*. International Society for Optics and Photonics, 2006, pp. 62 651U–62 651U.

[8] P. Hickson and R. Racine, "Image quality of liquid-mirror telescopes," *Publications of the Astronomical Society of the Pacific*, vol. 119, no. 854, p. 456, 2007.

[9] S. Thibault and E. F. Borra, "Liquid mirrors: a new technology for optical designers," *Optical Fabrication and Testing*, vol. 12, pp. 8–10, 1998.

[10] M. A. Covington, *How to Use a Computerized Telescope: Practical Amateur Astronomy*. Cambridge University Press, 2002, vol. 1.

[11] L. Sciavicco and B. Siciliano, *Modelling and control of robot manipulators*. Springer Science & Business Media, 2012.

[12] J. Denavit, "A kinematic notation for lower-pair mechanisms based on matrices," *ASME J. Appl. Mech.*, pp. 215–221, 1955.

[13] F. Reyes Cortes, F. R. Cortes, G. Rodriguez, M. M. G. Rodriguez, H. O. Moratto, H. O. Moratto, B. Kolman, D. R. B. Kolman, D. R. Hill, M. A. Montufar Benítez *et al.*, *MATLAB aplicado a Robotica y mecatronica*. e-libro, Corp., 2012, no. 681.51 670.4272.

[14] F. Reyes, *Robótica-Control de robots manipuladores*. Alfaomega Grupo Editor, 2011.

[15] M. W. Spong, S. Hutchinson, and M. Vidyasagar, *Robot modeling and control*. Wiley New York, 2006, vol. 3.

[16] A. G. Loukianov, "Robust block decomposition sliding mode control design," *Mathematical Problems in Engineering*, vol. 8, no. 4-5, pp. 349–365, 2002.

[17] P. D. Smith, *Practical astronomy with your calculator*. Cambridge University Press, 1981.

[18] C. E. Castañeda, A. G. Loukianov, E. N. Sanchez, and B. Castillo-Toledo, "Discrete-time neural sliding-mode block control for a dc motor with controlled flux," *IEEE Transactions on Industrial Electronics*, vol. 59, no. 2, pp. 1194–1207, 2012.

[19] O. A. Morfin, C. E. Castañeda, A. Valderrabano-Gonzalez, M. Hernandez-Gonzalez, and F. A. Valenzuela, "A real-time sosm super-twisting technique for a compound dc motor velocity controller," *Energies*, vol. 10, no. 9, p. 1286, 2017.

[20] H. K. Khalil, "Nonlinear systems. 2002," *ISBN*, vol. 130673897, p. 9780130673893, 2002.

[21] D. Hoffleit and C. Jaschek, "The bright star catalogue," *New Haven, Conn.: Yale University Observatory, c1991, 5th rev. ed., edited by Hoffleit, Dorrit; Jaschek, Carlos*, 1991.

Juan Cristobal Alcaraz Tapia received a Bachelor in Civil Engineer in 2015 from the Instituto Tecnológico Superior de Lagos de Moreno. He is studying for obtain a masters degree in applied Mathematics at Universidad de Guadalajara. His current research is focused on automatic control.

Carlos E. Castañeda received the B.S. in Communications and Electronics in 1995 from the Universidad de Guadalajara, México, the M.Sc. degree in Electronics and Computer Systems in 2003 from the Universidad la Salle Bajo, México, and the Ph. D. in Electrical Engineering in 2009 from CINVESTAV Guadalajara, México. He is working as Professor at Universidad de Guadalajara, Centro Universitario de los Lagos, México. His research interests are Automatic Control using artificial neural networks and Renewable Energy Sources.

Héctor Vargas Rodríguez is a Bachelor of Physics, 1994; Master in Theoretical Physics, 1998 and a Ph. D. in Physics, 2004; from the University Center of Exact Sciences and Engineering (CUCEI) of the University of Guadalajara, (U. de G.) 2004. Since 2006, he is an Associate Research Professor C assigned to the Department of Sciences Exact and Technology of the University Center of Los Lagos, U. de G. His current research are in relativistic physical effects in arbitrary reference frames and applied mathematics to the modelation of physical, electromechanical, biological, and social systems